Development of an Underwater Acoustic Communications Simulator

C.A. Hamm
M.L. Taillefer
Maritime Scientific Way Ltd

Prepared By:
Maritime Scientific Way Ltd
2110 Blue Willow Crescent
Orleans, ON K1W 1K3 Canada

Contractor's Document Number: AMBUSH.1.4
Contract Project Manager: C.A. Hamm, 613-824-6300
PWGSC Contract Number: W7707-145688
CSA: Stephane Blouin, DRDC - Atlantic Research Centre, 902-426-3100 x216

Contract Report
DRDC-RDDC-2015-C021
March 2014

Development of an Underwater Acoustic Communications Simulator

Contract Report # AMBUSH.1.4

Contract # W7707-145688

C.A. Hamm, M.L. Taillefer

Maritime Scientific Way Ltd (Ottawa, ON, Canada)

Fiscal Year 2013-2014

March 31 2014

This page intentionally left blank.

Table of contents

Table of contents i

List of figures ii

List of tables ii

1 Introduction 1

2 Simulator software 1

3 Simulator capabilities 2

4 Problems investigated 4

5 Effect of water currents 4

6 Effects of sea ice cover 6

7 Effects of wind generated waves 8

8 Summary and future work 10

Acknowledgements 11

References 12

List of figures

Figure 1: Context diagram of the simulator showing key inputs and outputs. . . . 1

Figure 2: Changes in computed channel impulse response due only to a change in current profile sampling density. 6

Figure 3: Full incoherent transmission loss field for 70% random distribution of ice cover. 7

Figure 4: Effect of increasing partial ice cover on arrival time spread and number of receive arrivals. 8

Figure 5: Scattering functions for 1s duration 14 kHz BPSK pulse for wind speeds 1, 5, 15 and 20 m/s, when no ice cover is present. 9

Figure 6: Scattering functions for 1s duration 14 kHz BPSK pulse for wind speeds 1, 5, 15 and 20 m/s, with a 50% randomly partial ice coverage. . 10

List of tables

1 Introduction

In order to achieve the development of a working underwater acoustic communications simulator in a short time span Maritime Way Scientific (MWS) chose to use existing open source software in association with our own signal, statistical, and control support Matlab scripts. The open source software is available online as part of the ONR's Ocean Acoustic Library (`http://oalib.hlsresearch.com/`), which is maintained by Heat, Light & Sound (HLS) Research, Inc., La Jolla, California. The open source models used by us are Bellhop and Virtex which were also developed by those at HLS. These models, along with our own scripts, allow coverage of a majority of the problems posed within the boundaries of this project.

2 Simulator software

This section describes the key software components of the simulator. The software is a combination of open source software and Maritime Way Scientific's own Matlab code which is used to control all software components and also provide support to creating simulator inputs and management and analysis of simulator outputs. A high-level view of the simulator is provided in Figure 1.

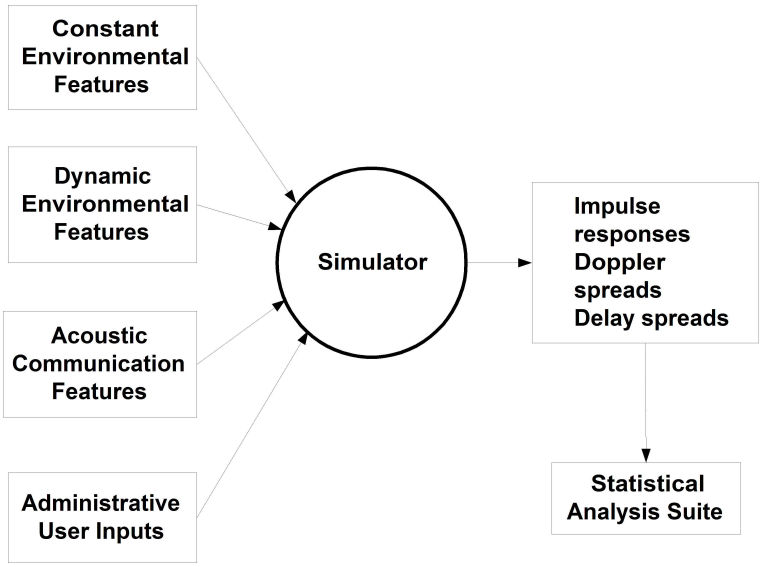

Figure 1: *Context diagram of the simulator showing key inputs and outputs.*

Bellhop is a Gaussian beam model, a ray formulation, which is particularly well suited to the high frequency (10-20 kHz) sonars in use for underwater modems. Bellhop is widely known and respected in the acoustic modelling community. Details on practical operation of Bellhop may be found in user manuals [1, 2] which also provide some insight into the

principles behind the technique used, without being too mathematical. The modems under consideration in this project, manufactured by Benthos, operate in the band 9 to 14 kHz. Bellhop is a fully range-dependent model which also allows altimetry to be defined for the air-water interface. This is particularly useful for the inclusion of sea ice. Bellhop, written in Fortran programming language, had to be modified in order to properly account for surface bounces which interacted with a solid-water interface (*i.e.*, ice boundary including shear speed and attenuation). Due to Bellhop being a ray-based model, it is able to compute the time-of-flight for each propagated ray, and these are assembled at the receiver position as the channel impulse response (arrivals structure). While Bellhop produces many types of standard model output (e.g. transmission loss) it is the arrivals structure and the eigenray trajectories (rays connecting only the source and receiver positions) which are required to compute the received time series in post processing. Normally this is as simple as convolving the transmitted signal with the channel impulse response. However, when including sea surface motion, or motion of source or receiver are in play, the arrival structure amplitudes and delays further corrections are needed to account for these perturbations.

Virtex [3] is a Matlab-based post-processor which computes the corrections to the Bellhop arrivals structure output. Virtex integrates dynamic sea surface motion, source and receiver motion, and an up-sampled version of the transmitted signal (e.g. as output by a modem), with the eigenray trajectories and arrivals structure, in order to compute the received signal at the receiver. This signal can be played over the computer audio or be made available for capture by another modem or recording device. As employed by us, Virtex calls the open source WAFO Matlab Toolbox [4] for generating spectrally accurate sea surfaces in range which changes over the duration of the signal transit in the channel. A sea surface may be generated with only wind speed being entered by the user. Virtex's use of WAFO for the problems encountered for this project necessitated several modifications and software fuses to prevent severe memory limit issues. Virtex was also modified by us to account for surface bounces which interact with the ice-water boundary.

3 Simulator capabilities

The following list summarizes the simulator capabilities.

- The simulator currently supports two main modes: Bellhop only and Virtex only. Each mode supports single-run and Monte Carlo runs so that some statistics may be gathered on the channel impulse response, or on the received signal due to waves and/or partial sea ice covers.
- Easy-to-use input files, as Matlab script templates are used to drive each mode of the simulator. In this approach the input file does not need to be parsed, but just simply loaded into Matlab's workspace.

- In Bellhop-only mode the input script contains: the administrative directory structure, the type of Bellhop output required (run sequentially), user can specify use of currents, their relative direction; use of ice cover and related parameters (surface altimetry etc.); bathymetry, maximum range and bottom type (via APL high-frequency ocean environmental acoustic handbook); signal frequency; source and receiver depth; sound speed profile; Monte Carlo of a fixed ice cover percentage; or an existing Bellhop input file; full reversal of the scenario environment for B-to-A communication; control of plotting outputs.

- In Virtex-only mode the input script contains: the administrative directory structure; identification Bellhop output files for defining the channel response; control over playing the propagated pulse sound; user can specify whether to use an ice cover or not; if using ice cover a batch of previously calculated ice keel depths may be identified, or newly created (batch runs over ice keel files, or single instances); ice cover statistics; wind speed and down swell wind spectral model; source and receiver speeds; reading of previously created signals or creation on-the-fly; input of signal creation parameters; reading of Dopplerized transmitted pulse replicas or created on-the-fly; selection of whether to calculate the scattering function or not; control of plotting outputs.

- The simulator script attempts to catch many user input errors or inconsistencies prior to launching deeply into what may be very lengthy calculations (minutes to hours for large batches).

- Virtex is extremely memory intensive. Software "fuses" have put in to manage and prevent memory lockups while maintaining a good level of fidelity.

- The scattering function [5, 6] which indicates each arrival and its Doppler shift on a Relative velocity vs. time 2D-plot.

- One-second duration continuous wave (CW) and binary phase shift key (BPSK) pulses with a centre frequency of 14.0 kHz have been propagated to 15 km under a time varying sea surface with partial ice cover, in the presence of water currents and sound speed stratification.

- Wave files (.wav) may be created for the input to the Virtex simulator. These mimic a digitally captured analog signal. Virtex outputs digital data which is converted to an audio file (signal) which could be passed to modem receiving electronics.

- Routines to determine basic signal statistics (spread, distribution, mean, median, rms level, standard deviation, skew, kurtosis).

4 Problems investigated

The following list summarizes the problems we have investigated in the course of the simulator development program:

- A mathematical basis for how water current affects the propagation calculation.
- Demonstrated the effects of water current on propagation and arrival structure. The greatest contributor is the current shear, since the Mach number, u/c, where u is the current speed and c is the speed of sound, is very small for natural water flow speeds. This was done with a new Matlab ray tracer which includes currents explicitly in the integration.
- Demonstrated the differences between calculating the ray trace with an exact implementation of the current correction versus a more simple 'summed' method (described below).
- Demonstrated how well a current profile must be sampled to maintain sufficient eigenray and channel response accuracy.
- Demonstrated the loss of acoustic reciprocity in the presence of water flow.
- Water current does not introduce Doppler. It primarily affects the time-of-flight along a ray path. Time-of-flight is used in acoustic tomography to determine current flows.
- Variation of the received signal due to wind speed.
- Variation of the channel impulse response due to variations in ice cover.
- Demonstration of large pulse-to-pulse variability.
- Doppler due to surface motion appears to be insignificant in comparison to source and receiver motion, except in very high winds (10-20 m/s).

5 Effect of water currents

There are several ways to express the speed of sound in moving media. One technique, shown in Thompson [7], was to derive the equivalent Snell's Law. Ray tracing may be performed by integrating the following equations with respect to x (equivalently, range):

$$\frac{dz}{dx} = \tan\alpha \text{ (ray depth versus range)} \tag{1}$$

and with the inclusion of current it can be shown that, for small Mach numbers ($M = u/c$),

$$\frac{d\alpha}{dx} = -\frac{c_z + U_z \sec\alpha}{c + U \sec\alpha} \text{ (ray launch angle versus range)} \tag{2}$$

where z is the depth in the water, α is the ray launch angle (from the horizontal, positive clockwise), c is the speed of sound (function of depth), U is the speed of water current (function of depth), and c_z and U_z are shorthand for vertical derivatives (gradients) dc/dz and dU/dz, respectively.

Note that for natural flows, the Mach number is very small, of order $M \approx 10/1500 << 1$, and so the $U \sec\alpha$ term in the denominator is quite small and serves mainly as a perturbation to the sound speed, and hence time-of-flight (about 0.5 ms/km per m/s of current). Sanford [8], provides insights with respect to the effects of current shear. The presence of the current gradient, U_z, in the numerator of equation (2) may be comparable to, or greater than, the sound speed gradient, c_z. This is significant as even in an isovelocity environment (i.e., $c_z = 0$) the current gradient remains which will refract sound, affecting the eigenrays which are found, and hence the channel impulse response is likewise affected.

Both equation (1) and equation (2) may form the basis of numerical ray tracing when currents are included. Implemented exactly, this integration must be carried out within the core of the propagation model. As the current, U, approaches zero equation (2) reduces to an approach as would be used in conventional ray tracing models that are derived for sound speeds depending only on depth. For moderate angles ($\alpha \leq 30^o$) equation (2) may be simplified to a "summed" sound-speed-plus-current approach, shown in equation (3),

$$\frac{d\alpha}{dx} = -\frac{(c+U)_z}{(c+U)} \tag{3}$$

In the numerator of equation (3) the sound speed (at depth z) and the current speed (at depth z) are summed, and then the vertical derivative is calculated. In the denominator only the sum is taken. The implications of this are that for moderate angles the current may be added to the sound speed profile outside of the model and then presented to the model as new sound speed profile: $c_{new} = c_{actual} + U$, without requiring changes to the propagation model code. As the water current is signed (i.e. $u < 0$ and $u \geq 0$) the introduction of water current leads to a loss of acoustic reciprocity in the channel. That is, the transmission loss calculated from A to B, is no longer the same as from B to A. Thus, in the presence of significant current (and its gradient) the simulator should be able to reverse the environmental inputs to calculate this B to A propagation, which we have implemented.

The exact approach (equations (1) and (2)) was compared to the summed approach (equations (1) and (3)) through the development of a range independent Matlab ray tracing algorithm which, for the purposes of ray tracing only, compared well to Bellhop. In his book "Computational Atmospheric Acoustics" Salomans discusses moving-medium effects [9].

For Mach numbers similar to, or larger than, our present case he demonstrates that the simple addition of the wind speed in the in-line direction was an accurate approximation. His tests included comparisons between a ray model and a Fast Field Program (FFP) method and found that in the frequency range of the ray theory, the results matched. We therefore conclude that the method using equation (3) is sufficient for use in the simulator as long as the current profile is sampled such that all significant current gradients are adequately resolved. Not capturing these current gradients will result in poor prediction performance.

The change in predicted channel impulse response due only to a more sparsely sampled current profile (evenly distributed samples) is demonstrated below in Figure 2. In Figure 2, from top to bottom, the number of evenly distributed data points over the full depth of 200 m, for an exponentially decaying sinusoidal current profile are 50 (true response), 30, 20, 10, respectively. The channel response change for each reduction in sampling density is clearly visible. This example shows that much later (erroneous) arrivals will be predicted than when the current function is fully sampled.

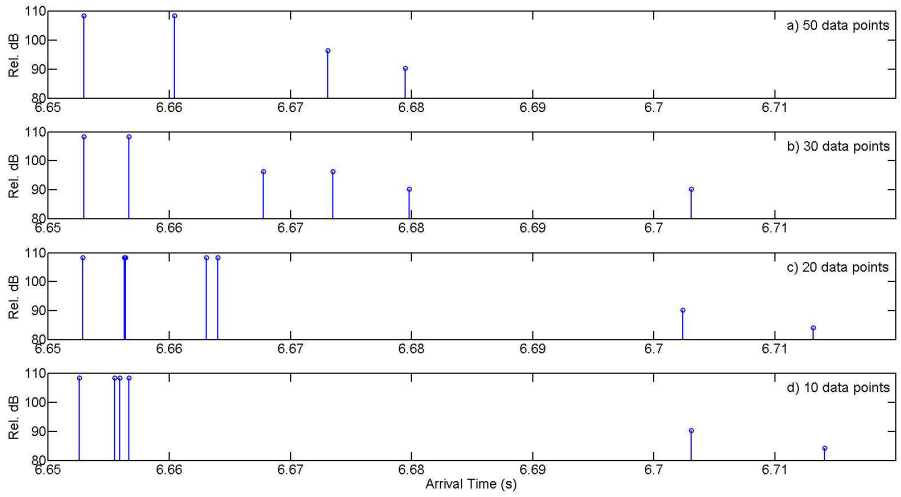

Figure 2: *Changes in computed channel impulse response due only to a change in current profile sampling density.*

6 Effects of sea ice cover

The initial results from a study on the effect of covering the sea surface with a partial canopy of sea ice are presented in this section. The Bellhop model is capable of accepting surface altimetry files. Thus, a simple algorithm was devised to create simple rough surfaces of random length (which serves as ice keels) separated by gaps (open leads) sea ice, with the percentage of partial coverage in range being controlled. While the ice keel model is not realistic at this time, however, we are of the opinion that the results will indicate the

general behavior of due to statistically generated surfaces. These data were used for the altimetry. Bellhop traces rays accounting for all bathymetry and surface altimetry. Therefore, the presence of small-scale surface altimetry, on the order of 1 m, affects the calculation of eigenrays hence the arrivals structure, or channel response. The eigenrays computed by Bellhop are also direct inputs to VirTEX, and therefore the computed received time series from VirTEX are directly affected by the ice canopy.

Figure 3 shows the Bellhop full-field (transmission loss at all depths and ranges) incoherent transmission loss calculation for a 14 kHz source located at zero range and 30 m depth. The sound speed is a linear upward-refracting profile with a gradient of 0.1 s-1. The colours indicate loss in decibels with values shown to the right of the plot. Thus, red indicates more sound energy (less loss) and blue indicates less sound energy (more loss). An ice canopy of 70% partial coverage augments the air-water interface. The mean ice keel draft is 2 m with a standard deviation of 0.5 m. Due to the plot scale, the partial ice canopy surface may be difficult for the reader to see. However, ranges with an ice canopy are easily located at the surface by observing the ribbons of higher sound energy (reflected by the air-water interface) as compared to the reflections by the solid ice (a lossy solid). This spatial banding of energy is an immediate consequence of the partial ice coverage. Due to the random nature of the ice keel lower surface the ice keels diffuse the sound energy upon reflection, as expected. A more detailed treatment of the effects of ice cover on transmission loss may be found in a recent paper by Alexander *et al.* [10].

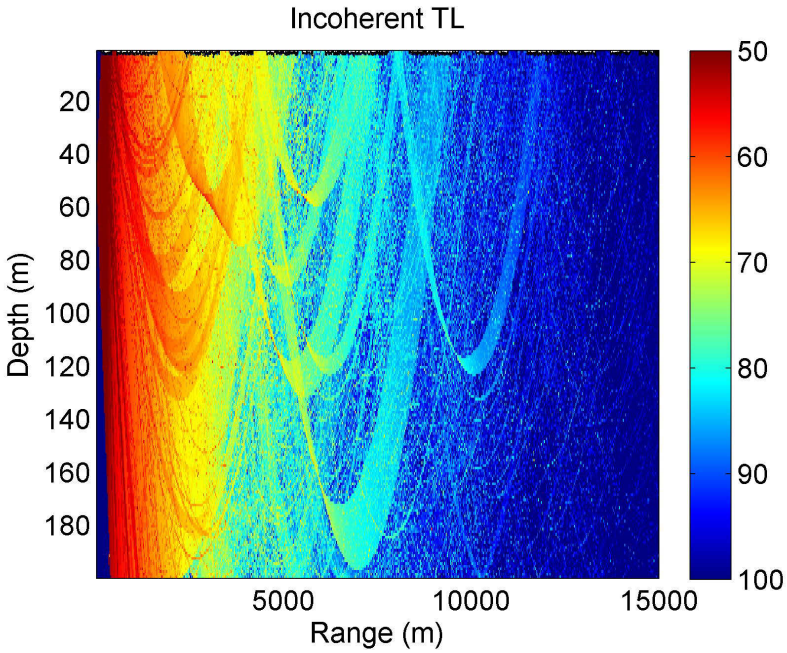

Figure 3: *Full incoherent transmission loss field for 70% random distribution of ice cover.*

The effects of partial ice cover on the time spread of arrivals and the number of arrivals (as determined by Bellhop) are summarized statistically in Figure 4. In the upper plot the

arrival spread, S_a, defined here as the time of the last delay less the time of the first delay ($t_{\text{delay max}} - t_{\text{delay min}}$), is shown for the case with no ice cover (solid black line) and for cases from 10% to 95% partial cover. To obtain these plots the arrival spread and number of arrivals from each of 100 generated instances of ice canopy were collected allowing histograms to be computed drawn and basic statistics (median, minimum, maximum, and standard deviation) extracted.

The mean value of the arrival spread (not shown) was close to the no-ice value, and the standard deviation from the mean (blue dashes) indicates only marginal variation from the mean. However, the delays of the latest arrivals (maximum, red dashes) were observed to notable increases in the arrival spread for all partial ice coverages, with up to 100% partial ice coverages of 70% and 95%. The number of arrivals, the lower plot of Figure 4, shows a substantial increase over the no ice case (22 arrivals) with up to 75 arrivals at 30% partial coverage, while the mean centres on about 40 arrivals. Based on the output of the Bellhop model the arrival structure is seen to clearly be influenced by, and is sensitive to, the introduction of partial ice covers.

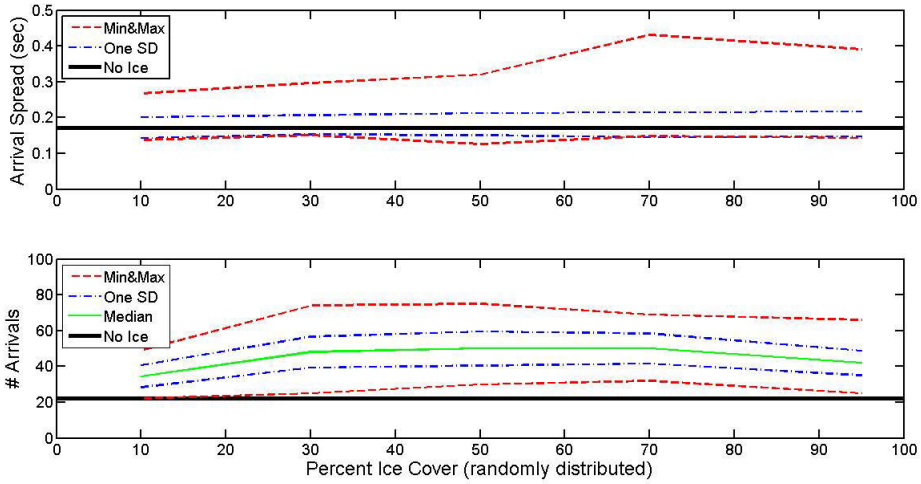

Figure 4: *Effect of increasing partial ice cover on arrival time spread and number of receive arrivals.*

7 Effects of wind generated waves

The simulator, as one of its post-processing options, calculates an estimate of the scattering function (hereafter, scattering function) [11]. Briefly, the transmitted signal is re-sampled and stretched (or compressed) in time over the range of anticipated Doppler velocities that may be encountered. This set of "pre-Dopplerized" waveforms are held in a library (a large file). The received signal, once propagated through the VirTEX algorithm, is then

time-reversed and correlated against each waveform held in the library file. Lags in the correlation (converted to delay time) which have a significant value indicate the arrival time and closest Doppler velocity estimate.

Figure 5, shows the scattering function for a BPSK signal with 1024 randomly assigned bits over 1 second, propagated through an isovelocity (1500 m/s) channel of depth 200 m when there is no ice surface altimetry at the surface. Source and receiver depths were 30 m and 100 m respectively. Wind speeds are 1, 5, 15 and 20 m/s, surface wave calculations employ the Pierson-Moskowitz wave spectrum [12]. The BPSK pulse is employed here, as in the work of Siderius and Porter [5] for its high Doppler sensitivity and ability to separate individual arrivals in the multipath environment. In each plot there are of order 10 or more correlated arrivals visible. Each image in Figure 5 indicates the scattering function from a single transmit ping. While there are ping to ping variations, in particular at higher wind speeds, these data are sufficient to illustrate the point that as the wind speed increases there is a commensurate deviation in the scattering function from zero Doppler velocity for the later arrivals. The earliest arrivals include direct path and bottom bounce and are unaffected by the surface. As later arrivals consist of high launch angle rays, as measured from the horizontal, they therefore probe the surface condition as they interact with the surface numerous times more so than lower launch angles. For wind speeds of 15 m/s to 20 m/s the calculated equivalent Doppler speeds introduced to the received signal are less than 1.5 m/s. This amount of Doppler shift is well below that which may be introduced by an autonomous underwater vehicle with onboard acoustic communications capability, communicating with an underwater sensor network.

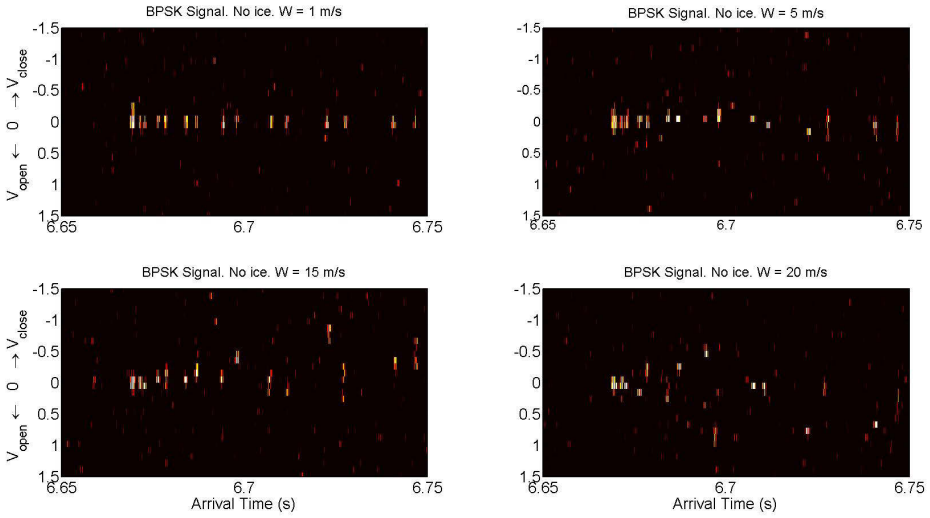

Figure 5: *Scattering functions for 1s duration 14 kHz BPSK pulse for wind speeds 1, 5, 15 and 20 m/s, when no ice cover is present.*

The images shown in Figure 6, below, illustrate the same scenario as in Figure 5 with the

addition of a 50% partial coverage of ice at the surface. First, note that the number of correlated arrivals in this situation is diminished from 10 (in Figure 5) to a range of three to six or seven, so that channel has become more sparse. Overall the same conclusions are drawn as for Figure 5), however it may be argued that the effect appears slightly diminished. Within our modified VirTEX eigenrays that interact with surface altimetry are shielded from the effects of the surface wave motion, and the ice position is fixed in space. The results shown in the images of Figure 6 appear to support this buffering by the presence of some ice canopy.

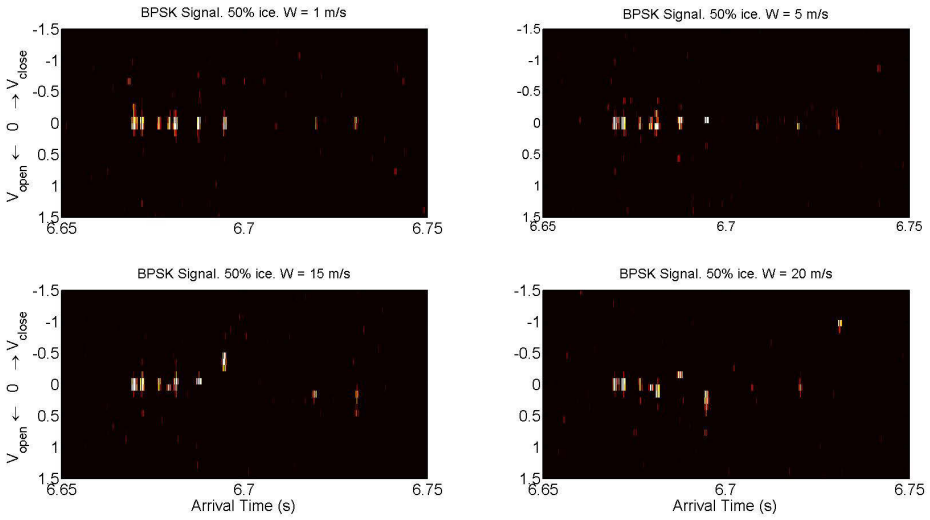

Figure 6: *Scattering functions for 1s duration 14 kHz BPSK pulse for wind speeds 1, 5, 15 and 20 m/s, with a 50% randomly partial ice coverage.*

8 Summary and future work

In a short period of time, the work presented here has resulted in a significant capability to probe the characteristics of shallow water channels. The main future tasks related to our simulator development is to develop the infrastructure that will permit integrating real (analog) signals into the simulation path, with full integration using underwater modems to occur in the final phase of this project. With respect to the current simulator, several enhancements should be considered. The statistical analysis of the simulator outputs should be better aligned to meet future needs, in particular, investigating network connectivity. Depending upon the chosen acoustic modems, the simulator could be extended and tested to longer pulses (1-3 seconds), other encoding schemes could be introduced, and with increased computer resources longer propagation ranges could be tested. Demodulation of VirTEX output, in order to determine message transmission integrity, should be considered. The simulator could be applied to the planning and affirmation of data acquired from field

experiments. Finally, to aid the users in all of these endeavors, a graphical user interface would further enhance usability.

Acknowledgements

The authors wish to thank Dr. Gary Brooke and Dr. Diana McCammon for their advice and assistance during the course of the project, in particular with respect to the effects of currents.

References

[1] Porter, M. B. (2011), The BELLHOP Manual and User's Guide: PRELIMINARY DRAFT.

[2] Rodriguez, O. C. (2008), General description of the BELLHOP ray tracing program.

[3] Peterson, J. C. and Porter, M. B. (2011), Virtual Timeseries EXperiment (VirTEX) - Quick Start.

[4] Brodtkorb, P., Johannesson, P., Lindgren, G., Rychlik, I., Rydén, J., and Sjö, E. (2000), WAFO - a Matlab toolbox for analysis of random waves and loads, In *Proc. 10th International Offshore and Polar Engineering conference*, Vol. 3, pp. 343–350, Seattle, USA.

[5] Siderius, M. and Porter, M. B. (2008), Modeling broadband ocean acoustic transmissions with time-varying sea surfaces, *J. Acoust. Soc. Am.*, 1(124).

[6] Peterson, J. C. and Porter, M. B. (2013), Ray/beam tracing for modeling the effects of ocean and platform dynamics, *IEEE Journal of Oceanic Engineering*, 38(4).

[7] Thompson, R. J. (1972), Ray theory for an inhomogeneous moving medium, *J. Acoust. Soc. Am.*, 5, part 2(51).

[8] Sanford, T. (1974), Observations of strong current shears in the deep ocean and some implications on sound rays, *J. Acoust. Soc. Am.*, 4(56).

[9] Salomans, E. M. (2001), Computational Atmospheric Acoustics, Kluwer Academic Publishers, Norwell, MA, USA. see section 4.6.

[10] Alexander, P., Duncan, A., N. Bose, N., and Smith, D. (2013), Modelling acoustic transmission loss due to sea ice cover, *Acoustics Australia*, 41(1).

[11] Proakis, J. (1995), Digital Communications, 3rd ed, McGraw-Hill, New York, NY.

[12] Jr., W. P. and Moskowitz, L. (1964), Proposed spectral form for fully developed wind seas based on the similarity theory of S.A. Kitaigorodskii, *Journal of Geophysical Research*, 69, 5181–5190.